3-1-2000

Structure-Enhanced Yield Stress of Magnetorheological Fluids

X. Tang

X. Zhang

R. Tao

Yiming Rong
Worcester Polytechnic Institute, rong@wpi.edu

Structure-enhanced yield stress of magnetorheological fluids

X. Tang, X. Zhang, and R. Tao[a)]
Department of Physics, Southern Illinois University, Carbondale, Illinois 62901-4401

Yiming Rong
Department of Mechanical Engineering, Worcester Polytechnic Institute, Worcester, Massachusetts 01609-2280

(Received 27 April 1999; accepted for publication 19 November 1999)

The yield stress of magnetorheological (MR) fluids depends on the induced solid structure. Since thick columns have a yield stress much higher than a single-chain structure, we improve the yield stress of MR fluids by changing the fluid microstructure. Immediately after a magnetic field is applied, we compress the MR fluid along the field direction. Scanning electron microscopy images show that particle chains are pushed together to form thick columns. The shear force measured after the compression shows that the structure-enhanced static yield stress can reach as high as 800 kPa under a moderate magnetic field, while the same MR fluid has a yield stress of 80 kPa without compression. This improved yield stress increases with the magnetic field and compression pressure and has an upper limit well above 800 kPa. The method may also be useful for electrorheological fluids. © *2000 American Institute of Physics.* [S0021-8979(00)02405-1]

I. INTRODUCTION

Magnetorheological (MR) fluids and electrorheological (ER) fluids have attracted considerable attention recently because of their wide applications, ranging from shock absorbers, clutches, engine mounts, flexible fixtures, to dynamically controlled systems.[1,2] A typical MR fluid consists of a suspension of solid magnetic particles of micrometer size in a liquid. Surfactants are added to alleviate the setting problem. Upon application of a magnetic field, the particles align in the field direction to form chains or clusters. As the magnetic field increases, MR fluid's yield stress is further strengthened. This process is reversible and the response time is in the order of milliseconds.

Currently, MR fluids have a typical yield shear stress around 80 kPa, exceeding the requirement for some mechanical application.[3] Therefore, MR fluids began to be employed in a few commercial devices.[4] On the other hand, current ER fluids have a yield stress around 10 kPa or below. Further development in ER materials is required for applications.

The yield stress produced by MR fluids under a magnetic field is the key parameter for applications. Ginder and Davis predicted that the yield stress of an iron-based MR fluid at 50% volume fraction was capped at 200 kPa. Their calculation was based on single-chain structure and took magnetic saturation into account.[5] The prediction would be correct if magnetic particles in MR fluids only form a single-chain structure.[6,7] On the other hand, many applications require that MR fluids have a yield stress much stronger than 200 kPa, such as flexible fixtures for manufacturing. To increase the yield stress of MR fluids, especially, to have a strong yield stress at low magnetic field is important for applications, but presents a challenge. Can MR fluids have a yield stress exceeding 200 kPa? In this article, we present a new approach that makes MR fluids super strong. We start from improving the microstructure of MR fluids under a magnetic field to obtaining the static yield stress exceeding 800 kPa.

It is well known now that under a strong magnetic (or electric) field, the ideal structure of MR (or ER) fluids is a body-centered-tetragonal (bct) lattice.[8–10] The yield stress of MR fluids strongly depends on the microstructure, how magnetic particles are arranged in a magnetic field. For example, a bct lattice has a much higher yield stress than a single-chain structure.[11] Experiments on steel balls with different structure arrangements also support this point.[12] Therefore, if we can change the single-chain structure to thick column structure, MR fluids will have a much strong yield stress. On the other hand, when a magnetic field is applied to a MR fluid, the magnetic particles first form chains. The natural aggregation from single-chain structure to thick columns is a slow process[13] and not helpful. Therefore, we must rely on other alternative.

Based on this knowledge, we seek a new approach to produce structure-enhanced yield stress. Immediately after a magnetic field is applied, we compress the MR fluid before a shear force is applied. The magnetic field produces chains in milliseconds. The compression pushes these chains together to form a close-packed cluster. Our scanning electron microscopy (SEM) images show that particle chains are indeed pushed together to form thick columns. This fluid structure change greatly enhances the yield stress. Our experiments on an iron-based MR fluid find that this structure-enhanced static yield stress can reach as high as 800 kPa, ten times of the yield stress without compression. When the magnetic field is removed, the MR fluid still returns to the liquid state quickly. The upper limit of this structure-enhanced yield stress seems well above 800 kPa. We expect that this method and the physics principle are applicable to ER fluids as well.

a)Electronic mail: rtao@physics.siu.edu

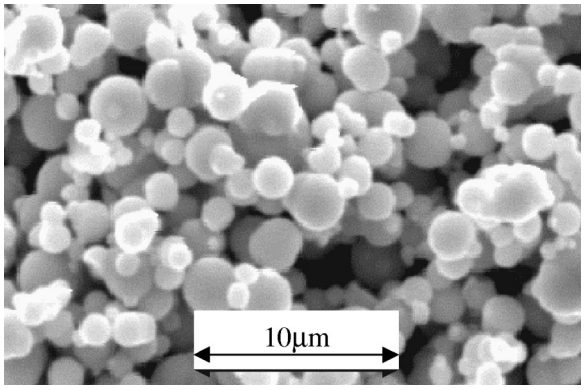

FIG. 1. SEM image of carbonyl iron particles.

The super-strong MR and ER fluids developed with this method will be suitable for many applications. For example, the structure-enhanced yield stress of MR fluids is now strong enough for flexible fixture in manufacturing industry.

II. EXPERIMENTS

We used a suspension of carbonyl iron particles (SIGMA Chemical Co) in silicone oil with a volume fraction 46%–50% in our experiment. As shown in the SEM image (Fig. 1), the carbonyl iron particles are spherical with average diameter around 4.5 μm. The silicone oil has viscosity 0.05 poise. A small amount of surfactant was added into the suspension so that the particles could suspend in silicon oil without settling for at least 24 h. The surfactant was quite viscous, bringing the zero-field viscosity of our fluid to about 10 poises.

The experimental setup is in Fig. 2. An electromagnet with two water-cooled coils produced a magnetic field in the horizontal direction. The aluminum container between the two magnet poles had one sliding iron wedge and one fixed guiding iron wedge at each side close to the magnetic poles. The interface between the sliding wedge and the guiding wedge had a 12° angle to the vertical direction. As the sliding wedges were pushed down, the MR fluid was compressed in the field direction. The container had a height 115 mm and a square horizontal cross section, 89 mm×89 mm, providing a volume 200 ml. We poured 120 ml MR fluid into the container. Before the application of magnetic field, we inserted an aluminum bar vertically into the container center. Then, a magnetic field is applied to solidify the MR fluid. Immediately, we compressed the MR fluid by pushing the two sliding wedges down symmetrically. As the sliding wedges went down, the MR fluid's level rose. To determine the yield stress, we attached a force transducer (Model 3185-500) and a strain gauge conditioner-amplifier (Model 3170, Daytronic Co.) to pull the test bar out. The MR fluid's yield stress was very strong. We had to use a screw-driven linear slider to generate sufficient force to extract the test bar. In order to measure the compression pressure inside the MR fluid, we used four strain gauges (FLA-5-11, Tokyo Sokki Kenkyujo Co., Ltd) on the surfaces of the test bar to form a typical Wheatstone bridge circuit, which enabled us to find the equivalent *in situ* normal stress P_e. The yield stress depends on the applied magnetic fields and the compression pressure.

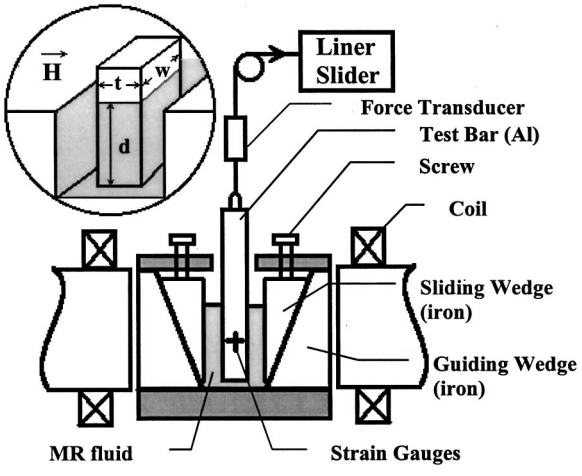

FIG. 2. Experimental setup.

To decide the modulus, we also needed the test bar's vertical displacement under force. The displacement was very tiny before the MR fluid had yielded. We attached a small mirror to the test bar. A tiny displacement led to a small rotation of the mirror. From the laser beam deflected by the mirror, we could determine the displacement with accuracy of 1 μm. This displacement is so small that the tensile elongation of the test bar must be subtracted to obtain a correct shear strain. On the other hand, the post-yield displacement was not tiny. Instead of laser beam, we used a spring micrometer (L. S. Starrett Co.) to measure it.

The test bar's cross section is rectangle. We denote the side perpendicular to the field as w and the side parallel to the field as t. The depth of the bar submerged in the MR fluid is d. The bottom area is $A_b = wt$. The areas perpendicular to the field or parallel to the field submerged in the MR fluid are $A_\perp = 2wd$ and $A_\parallel = 2td$, respectively. The vertical force F_t needed to pull out the test bar is given by

$$F_t = \tau_\perp A_\perp + \tau_\parallel A_\parallel + p_0 A_b + mg', \tag{1}$$

where $\tau_\perp$ and $\tau_\parallel$ are the yield stress on a plane perpendicular to the field direction or on a plane parallel to the field direction, respectively, p_0 is the atmosphere pressure, and mg' is the bar's weight minus the buoyancy. The last two terms are quite small. We define $F_{\mathrm{MR}} = F_t - p_0 A_b - mg' = \tau_\perp A_\perp + \tau_\parallel A_\parallel$ as the net MR pullout force. By varying the size of $A_\perp$ and $A_\parallel$, we determined $\tau_\perp$ and $\tau_\parallel$. In our experiment, the four aluminum bars had $t = 1/2$ in., but $w = 1$, 1/2, 1/4, and 1/8 in., respectively. The leading term in F_{MR} is $\tau_\perp A_\perp$.

Since the test bar is nonmagnetic, the field around the bar is not uniform. The field H_1 at the front center of the test bar was less than the field H_2 at the side parallel to the field. As it was difficult to measure the field inside the MR fluid and the tangential component of magnetic field is continuous at any interface that has no surface current, we measured H_1 and H_2 at the MR fluid surface. Table I shows H_1 and H_2 for a test bar with $t = 1/2$ in. and $w = 1$ in. As the coil current increases, the ratio H_2/H_1 drops from 1.85 at 1 A to 1.30 at

TABLE I. Relationship between the coil currents and the magnetic field.

Coil current I (A)	1.0	2.0	3.0	4.0	5.0	6.0	7.0	8.0	9.0
Field H_1 (kA/m)	37.6	103	187	250	306	350	388	418	445
Field H_2 (kA/m)	69.6	188	289	370	440	486	526	558	582
Mean field H (kA/m)	53.6	146	238	310	373	418	458	488	514
Ratio H_2/H_1	1.85	1.82	1.54	1.48	1.44	1.39	1.36	1.34	1.31

9 A. For simplification, we take average $H=(H2+H_1)/2$ as the mean value of H in our calculation.

Figure 3 shows F_{MR} versus the compression for a test bar with $t=1/2$ in. and $w=1$ in. It is clear that F_{MR} increases linearly with the compression pressure. Hence, the yield shear stress $\tau_{y(H)}$ increases with the normal stress P_e. Through each measurement, the normal stress P_e and the magnetic field remain fixed. An empirical expression is given by

$$\tau_{y(H)}=\tau_0+K_{(h)}P_e, \tag{2}$$

where τ_0 is the yield stress of MR fluid without compression. The slope $K_{(h)}$ increases with the field H, from 0.221 for $H=238$ kA/m, 0.239 for $H=372$ kA/m, to 0.267 for $H=458$ kA/m. The relationship in Eq. (2) holds for test bars of different size. With a small test bar, we obtained a static yield shear stress exceeding 800 kPa. As shown in Fig. 3, the increase of yield stress with the compression pressure is linear and there is no sign of saturation. The point of saturation is beyond the capacity of our current measurement.

Figure 4 shows the effect of magnetic field on the yield stress. The MR fluid without compression has a static yield shear stress around 80 kPa at $H=372$ kA/m and 120 kPa at $H=514$ kA/m. The other two curves of compressed MR fluid were obtained as follows. We first applied a magnetic field of 372 kA/m, then compressed the MR fluid with a normal stress of 1.2 or 2.0 MPa, respectively. Afterwards, we varied the coil current and measured the pullout force at various magnetic fields. During the experiment, we always gave at least 30 s for the MR fluid to relax after compression or change of magnetic field. Figure 4 clearly indicates that the yield stress is greatly enhanced by the compression. Reducing the magnetic field below 50 kA/m after the compression led to a sharp drop of the yield stress.

The internal pressure inside the MR fluid is not uniform under compression. During the experiment, we monitored the pressure on the test bar at its middle point. We noted that the built-up pressure under compression was also reduced at a low field as the yield stress had a drop. When the magnetic field was off, the MR fluid had a residual yield stress 20–40 kPa and a residual field less than 0.5 kA/m. This hysteresis indicates that the magnetic particles formed a solid structure under the compression and the solid structure remained after the external field was removed. However, this hysteresis was so weak that a light stir returned the MR fluid back to its liquid state immediately.

Figure 5 shows the relationship between the shear stress and shear strain. The magnetic field was 372 kA/m for all cases. Without compression, the MR fluid began to yield at a shear stress 20 kPa. The elastic modulus was about 10^7 Pa. After the yield point, the shear stress increases gradually until it reaches a maximum 80 kPa at a shear strain 0.35. With the compression, the MR fluid became much stronger and more rigid. The elastic limit, the modulus, and the yield stress were all increased dramatically. The overshoot of

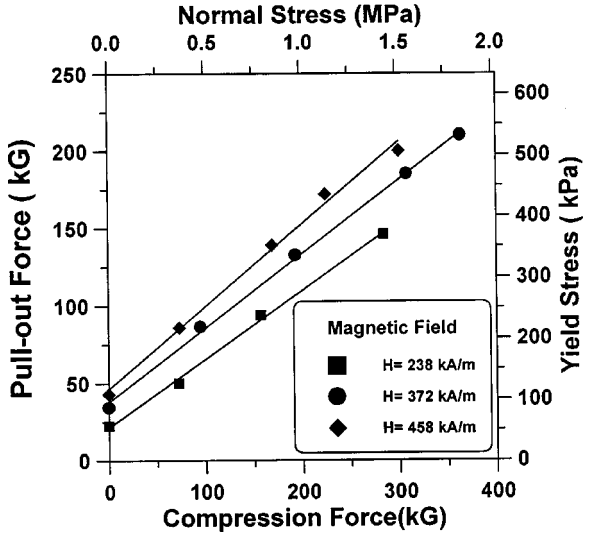

FIG. 3. Yield shear stress of the MR fluid linearly increases with the normal stress.

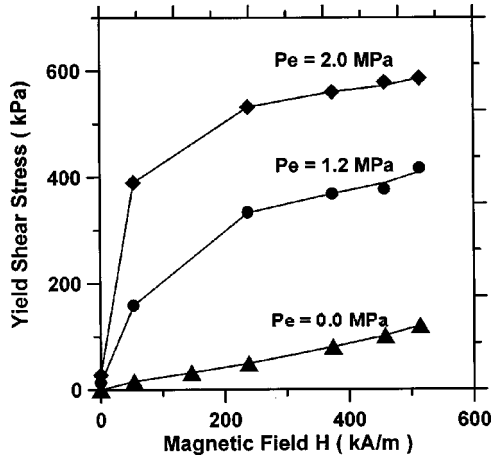

FIG. 4. Yield stress versus magnetic field with and without compression. The compression was taken under magnetic field of 372 kA/m. The variation of field was performed afterwards.

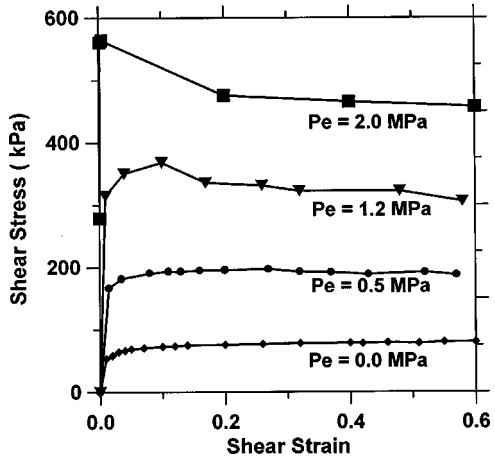

FIG. 5. Relationship between shear stress and shear strain with and without compression. The magnetic field is 372 kA/m for all cases.

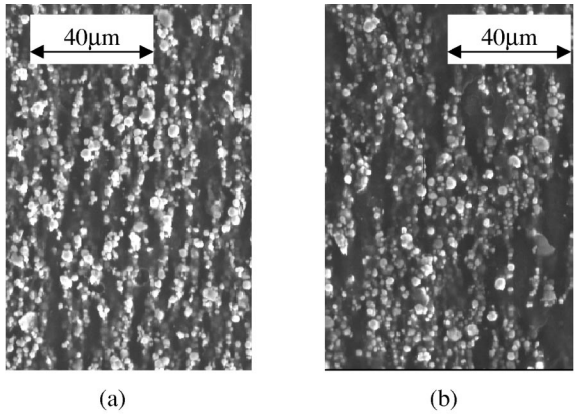

FIG. 6. SEM images of iron–epoxy mixtures cured under magnetic field of 372 kA/m. The field direction is upwards in the diagrams. (a) Without compression. (b) With compression at 1.2 MPa. The compression changes the single-chain structure to thick columns.

shear stress occurred at high compression pressure, indicating that the yielding process is sensitive to a structure change. A large shear strain breaks the microstructure of MR fluids and leads to a sharp decrease of shear stress. At $P_e = 2.0\,\mathrm{MPa}$, the shear modulus is as high as 5.0×10^8 Pa, 2% of aluminum's shear modulus. It is also worthwhile to mention that the structure-enhanced strength of MR fluids is very stable. The shear modulus does not change in 24 h after the compression as long as the magnetic field holds the fluid.

From the rising fluid level and the moving wedge down position, we note that our fluid has small compressibility. This is because there were some air bubbles inside the MR fluid. We used a vacuum pump to extract air bubbles from the MR fluids before the experiment. This made the experiment repeatable. However, we could not get rid all air bubbles. The maximum compressibility ratio of the fluid was 1.5% when the fluid was compressed at $H = 372\,\mathrm{kA/m}$ and pressure 2.0 MPa.

III. MICROSTRUCTURE

To understand the physical mechanisms underlining this yield stress enhancement, we examined the microstructure of MR fluid before and after the compression. To do so, instead of silicon oil, we used polymer resins (Epoxy) to mix with iron particles at 45% volume fraction. Then, we applied a magnetic field of 372 kA/m on the new irreversible MR fluid. The resin had one-hour cure time. In one process, we did not compress the fluid and let resin solidify. In another process, we compressed the MR fluid with a pressure of 1.2 MPa and let the resin solidify under pressure. Afterwards, we cut the cured solid pieces with a diamond saw and conducted SEM analysis. Figure 6(a) shows the microstructure of MR fluid without compression. Figure 6(b) is the microstructure of MR fluid under compression. It is clear that without the compression, MR fluid's microstructure was dominant by single chains. As our particles were not uniform, chains were not perfect, either, but all of them were not very thick. As shown in Fig. 6(b), MR fluid's microstructure changed into thick columns after the compression. The average column thickness was over 50 μm, implying that one column had at least 100 particles or more in its cross section. When a magnetic field is applied, magnetic particles quickly form chains. Natural aggregation from single chains to thick columns is not only slow, but also produces columns with very limited thickness. As we compress the MR fluid, chains get shorter and are pushed close to form a close-packed structure, probably a BCT-lattice based structure, which has a much high yield stress and modulus. The columns produced by compression are thicker and stronger than the product of natural aggregation.

The microstructure structure is the key to the enhancement of yield stress. In another experiment, we change the process order: compress the MR fluid before application of magnetic field. Such process does not produce any yield stress enhancement. The reason is easy to understand. Before application of magnetic field, the magnetic particles can move freely within the base liquid. Compression before the formation of solid structure does not create thick columns. Therefore, there is no change of yield stress.

Once solid structure is formed in the MR fluid, the normal pressure is no longer uniform within the fluid. Our compression thus also increases the friction between the MR particles and the test bar's surface as the friction is proportional to the normal pressure. We note that the yield stress of our compressed MR fluid has a sharp drop as the magnetic field is reduced below 50 kA/m (Fig. 4). This may also due to the nonuniform internal pressure. During the compression, close-packed structures are formed and the local internal pressure difference is also increased. When the magnetic field is reduced to below 50 kA/m, the magnetic force is no longer sufficient to resist the local pressure difference and the particles begin to move to rearrange themselves. Our experiment thus also records a sharp decrease of the normal stress. This brings a sharp decrease of the yield stress.

IV. DISCUSSIONS

Finally, we would like to mention that the empirical Eq. (2) is consistent with Mohr–Coulomb theory.[13,14] Coulomb first showed that the yield shear stress should linearly increase with the normal stress. Let us denote the MR fluid's

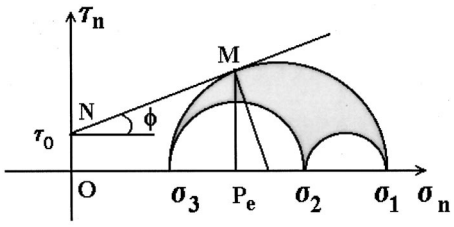

FIG. 7. Mohr-circle diagram to find the limiting stress. ON represents τ_0 and NM is tangential to the biggest circle.

stress tensor by τ_{ij} $(i,j=1,2,3)$ that is a combination of the mechanical tensor and Maxwell tensor.[15] The normal stress σ_n and shear stress τ_n on the plane with a normal direction **n** are given as follows:

$$\sigma_n=\Sigma_{ij}\tau_{ij}n_in_j, \tag{3}$$

$$\sigma_n^2+\tau_n^2=\Sigma_{ijl}\tau_{ij}\tau_{il}n_jn_l. \tag{4}$$

If τ_{ij} has three principal values $\sigma_1\geqslant\sigma_2\geqslant\sigma_3$, and the three components of the unit vector **n** to the three principal axes are still denoted by n_i $(i=1,2,3)$, then Eqs. (3) and (4) can be written as

$$\sigma_n=\sigma_1n_1^2+\sigma_2n_2^2+\sigma_3n_3^2, \tag{5}$$

$$\sigma_n^2+\tau_n^2=\sigma_1^2n_1^2+\sigma_2^2n_2^2+\sigma_3^2n_3^2. \tag{6}$$

If we use the points $(\sigma_2+\sigma_3)/2$, $(\sigma_1+\sigma_3)/2$, $(\sigma_1+\sigma_2)/2$ as the centers and $(\sigma_2-\sigma_3)/2$, $(\sigma_1-\sigma_3)/2$, $(\sigma_1-\sigma_2)/2$ as the radii to draw Mohr circles (Fig. 7), the area confined by the large and two small circles defines all possible values of σ_n and τ_n. As mentioned before, τ_0 is the yield stress without compression, represented by *ON*. The maximum allowed value of τ_n is represented by a point *M*, where the line *NM* is tangential to the biggest circle. Hence, the maximum shear stress τ_y is approximately expressed by

$$\tau_y=\tau_0+\sigma_n\tan\phi. \tag{7}$$

Also from Coulomb's argument, ϕ is the angle of internal friction. If we note that P_e in Eq. (2) is just σ_n here, then, for example, $\tan\phi=K_{(h)}=0.239$ or $\phi=13.44°$ at $H=372$ kA/m. The values of ϕ and the internal friction coefficient $\tan\phi$ seem to be reasonable. As mentioned before, $K_{(h)}$ increases with the magnetic field slightly. Then, the internal friction seems to increase slightly with the magnetic field.

The test bar in our experiment is made of nonmagnetic material (aluminum alloy); the ''wall effect'' may underestimate the yield stress of MR fluid.[16,17] However, the average MR particle size 5 μm (Fig. 1) is much smaller than the bar's surface roughness ($\sim$30 μm). There is no reason to believe that the MR particles could slip on the surface. To verify this, we also conducted an experiment with a steel bar. There was no significant change in the results of yield stress. On the other hand, it is very difficult to align a steel bar in a high magnetic field. For future applications, we decided to use aluminum bar throughout our experiment.

To conclude this article, we expect that the current approach is applicable for ER fluids. If the structure-enhanced yield stress of ER fluids can also be ten times higher than the yield stress without compression, this method will enable ER fluids to have a yield stress exceeding 50 kPa, strong enough for many industrial applications.

ACKNOWLEDGMENTS

The authors wish to thank M. Khan, T. Essery, and J. Yu for their assistance. This research is supported by NSF Grant No. SGER-9725012 and a grant from MTC of SIUC. One of the author's (X. T.) work was partially supported by NNSFC Grant Nos. 19772049 and 19834020.

[1] For example, see *Electrorheological Fluids, Magnetorheological Suspensions and their Applications*, edited by M. Nakano and K. Koyama (World Scientific, Singapore, 1999); *Electrorheological Fluids, Magnetorheological Suspensions and Associated Technology*, edited by W. A. Bullough (World Scientific, Singapore, 1996); *Electrorheological Fluids*, edited by R. Tao and G. D. Roy (World Scientific, Singapore, 1994).
[2] J. D. Carlson and M. J. Chrzan, U.S. Patent No. 5 277 282 (1994), J. D. Carlson, M. J. Chrzan, and F. O. James, U.S. Patent No. 5 284 330 (1994); O. Ashour, C. A. Rogers, and W. Kordonsky, J. Intell. Mater. Syst. Struct. **7**, 123 (1996).
[3] D. I. Hartsock, R. F. Novak, and G. J. Chaundy, J. Rheol. **35**, 1305 (1991).
[4] J. D. Carlson, D. M. Catanzarite, and K. A. St. Clair, Int. J. Mod. Phys. B **10**, 2857 (1996); W. I. Kordonsky and S. D. Jacobs, *ibid.* **10**, 2837 (1996).
[5] J. M. Ginder and L. C. Davis, Appl. Phys. Lett. **65**, 3410 (1994).
[6] P. P. Phule and J. M. Ginder, in *Electrorheological Fluids, Magnetorheological Suspensions and their Applications*, edited by M. Nakano and K. Koyama (World Scientific, Singapore, 1999), p. 445.
[7] J. M. Ginder and J. L. Sproston, *Proceedings of the Fifth International Conference On New Actuators*, edited by H. Borgmann (Axon Technologie Constult, Bremen, Germany, 1996), p. 313.
[8] R. Tao and J. M. Sun, Phys. Rev. Lett. **67**, 398 (1991).
[9] T. J. Chen, R. N. Zitter, and R. Tao, Phys. Rev. Lett. **68**, 2555 (1992).
[10] L. Zhou, W. Wen, and P. Sheng, Phys. Rev. Lett. **81**, 1509 (1998).
[11] G. L. Gulley and R. Tao, Phys. Rev. E **48**, 2744 (1993).
[12] X. Tang, Y. Chen, and H. Conrad, J. Intell. Mater. Syst. Struct. **7**, 517 (1996).
[13] S. S. Vyalov, *Rheological Fundamentals of Soil Mechanics* (Elsevier, New York, 1986), pp. 100–107.
[14] J. J. Tuma and M. Abdel-Hady, *Engineering Soil Mechanics* (Prentice–Hall, Englewood Cliffs, NJ, 1973), pp. 207–209.
[15] R. E. Rosensweig, J. Rheol. **39**, 179 (1995).
[16] E. Lemaire and G. Bossis, J. Phys. D **24**, 1473 (1991).
[17] T. Miyamoto and M. Ota, Appl. Phys. Lett. **64**, 1165 (1994).